

Modern erosion rates in the High Himalayas of Nepal

Emmanuel J. Gabet^{a,*}, Douglas W. Burbank^b, Beth Pratt-Sitaula^c,
Jaakko Putkonen^d, Bodo Bookhagen^e

^a Department of Geology, San Jose State University, San Jose, CA 95192, USA

^b Department of Geological Sciences, University of California, Santa Barbara, CA 93106, USA

^c Department of Geological Sciences, Central Washington University, Ellensburg, WA 98926, USA

^d Department of Earth and Space Sciences, University of Washington, Seattle, WA 98195, USA

^e Geological and Environmental Sciences, Stanford University, Stanford, CA 94305, USA

Received 25 June 2007; received in revised form 29 November 2007; accepted 30 November 2007

Available online 15 December 2007

Editor: H. Elderfield

Abstract

Current theories regarding the connections and feedbacks between surface and tectonic processes are predicated on the assumption that higher rainfall causes more rapid erosion. To test this assumption in a tectonically active landscape, a network of 10 river monitoring stations was established in the High Himalayas of central Nepal across a steep rainfall gradient. Suspended sediment flux was calculated from sampled suspended sediment concentrations and discharge rating curves. Accounting for solute and bedload contributions, the suspended sediment fluxes were used to calculate watershed-scale erosion rates that were then compared to monsoon precipitation and specific discharge. We find that, in individual watersheds, annual erosion rates increase with runoff. In addition, our data suggest average erosion rate increases with discharge and precipitation across the entire field site such that the wetter southern watersheds are eroding faster than the drier northern watersheds. The spatially non-uniform contemporary erosion rates documented here are at odds with other studies that have found spatially uniform long-term rates (10^5 – 10^6 yr) across the pronounced rainfall gradient observed in the region. The discrepancy between the modern rates measured here and the long-term rates may be reconciled by considering the high erosional efficiency of glaciers. The northern catchments were much more extensively glacierized during the Pleistocene, and therefore, they likely experienced erosion rates that were significantly higher than the modern rates. We propose that, in the northern watersheds, the high rates of erosion during periods of glaciation compensate for the low rates during interglacials to produce a time-averaged rate comparable to the landslide-dominated southern catchments.

© 2007 Elsevier B.V. All rights reserved.

Keywords: Himalayas; Nepal; erosion; suspended sediment; climate

1. Introduction

A current theory in geology proposes a strong linkage between tectonics, climate, and erosion (Beaumont et al., 2001; Hodges et al., 2001; Hodges et al., 2004; Wobus et al., 2003). According to this hypothesis, surface uplift of the Himalayas causes orographic precipitation that focuses erosion at the southern range front. Erosional unloading, in turn, is interpreted

to localize tectonic strain and control the location of thrust faults (Beaumont et al., 2001; Hodges et al., 2001; Hodges et al., 2004; Wobus et al., 2003). Inherent in this argument is the assumption that erosion increases with precipitation (Reiners et al., 2003). Indeed, Thiede et al. (2004) measured exhumation rates along the Himalayan front in India and found that the highest rates were in the region of highest precipitation. In contrast, others (Burbank et al., 2003) have suggested that at the time-scale of 10^5 – 10^6 yr, erosion rates in the Himalayas are driven primarily by tectonic rates. This hypothesis is supported by approximately uniform fission-track ages along a north–south transect in central Nepal that crosses the Greater Himalaya and

* Corresponding author. Tel.: +1 408 924 5035; fax: +1 408 924 5053.

E-mail address: egabet@email.sjsu.edu (E.J. Gabet).

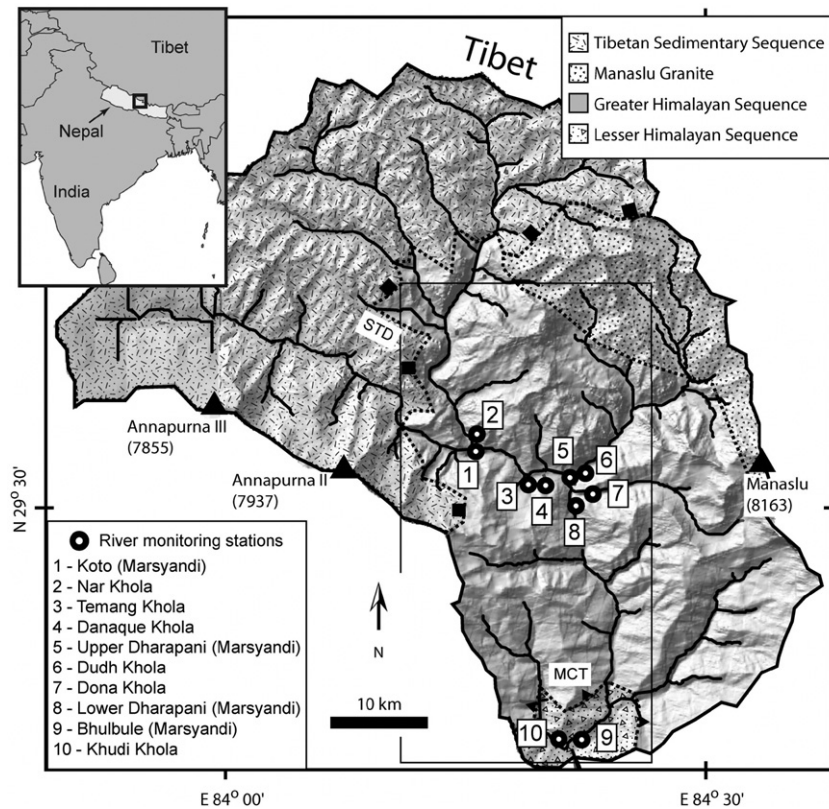


Fig. 1. Shaded-relief map of the Annapurna watershed with monitoring stations. Lithological map modified from Searle and Godin (2003). Dotted lines delineate lithological contacts. The location of the two major fault systems are shown (MCT = Main Central Thrust; STD = Southern Tibetan Detachment). Rectangle in main map delineates area covered by weather station network (see Fig. 2). Khola = river.

spans an order-of-magnitude increase in precipitation rates (Blythe et al., 2007; Burbank et al., 2003; Whipp et al., 2007).

Because most erosional processes are dependent on flowing water (e.g., landslides and bedrock channel incision), annual precipitation is often invoked as having a first-order control on rates of denudation. Whereas some have found a relationship between runoff (a proxy for precipitation) and erosion (e.g., Milliman and Syvitski, 1992), studies that have specifically focused on tectonically active mountain ranges have generally failed to find a correlation. For example, Riebe et al. (2001) concluded that climate had only a weak control on erosion in catchments in the Sierra Nevada of California, despite a nearly order-of-magnitude difference in precipitation across the study area. Similarly, after analyzing sediment flux records from 47 catchments in the Andes, Aalto et al. (2006) failed to find a relationship between denudation and runoff. Instead, Aalto et al. (2006) concluded that erosion rates were positively correlated to average basin slope and relief. The dominant role of topography in controlling erosion rates in mountainous landscapes has also been supported by Montgomery and Brandon (2002) in the Cascade Range of Washington State (USA), Schaller et al. (2001) in Europe, and Vance et al. (2003) in the Upper Ganges catchment in Nepal.

To explore potential relationships between climate, erosion, tectonics, and topography, we initiated a project in the Annapurna–Manaslu region of Nepal (Fig. 1). Between 2000 and 2002, a

network of 10 river-gauging stations was established along the Marsyandi River and 6 of its tributaries. Over the next 5 yrs, the stations were monitored during the monsoon season for measuring discharge and suspended sediment concentrations in order to calculate suspended sediment fluxes and, by inference, the basin-averaged erosion rates. These river monitoring stations complemented a network of established meteorological stations (Barros et al., 2000; Putkonen, 2004). This provided an opportunity to compare erosion rates and climatic variables at the same temporal scale: whereas erosion in the Himalayas can be measured at various time scales, from the present to the past 10^7 yr (e.g., Ruhl and Hodges, 2005), accurate measurements of precipitation can only be made for the present.

2. Material and methods

2.1. Field site

The study region spans the breadth of the High Himalayas in central Nepal and reaches into the Tibetan Plateau (Fig. 1). This area is one of the wettest in the High Himalayas (Bookhagen and Burbank, 2006) and has a striking precipitation gradient: weather station data (Barros et al., 2000; Burbank et al., 2003; Gabet et al., 2004c; Putkonen, 2004) indicate a ten-fold decrease in monsoon rainfall (4500 to 350 mm/yr) along a 40-km, south-to-north transect (Fig. 2). The southern portion of

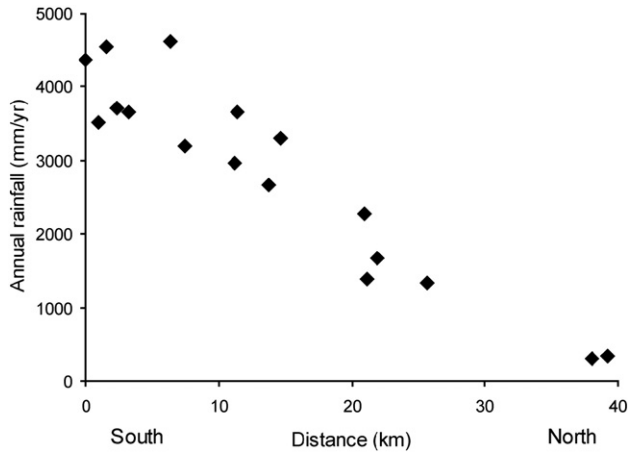


Fig. 2. South–north precipitation transect (see Fig. 1). Rainfall data from a network of meteorological stations show a steep decline in annual rainfall across the High Himalayas.

the field area is underlain by schists, limestones, and quartzites of the Lesser Himalayan series (Fig. 1). The middle portion is dominated by gneisses of the Greater Himalayan series and the northern portion is underlain by sedimentary units of the Tethyan series (Colchen et al., 1986). The field site is divided by two main fault zones, the Main Central Thrust in the south and the Southern Tibetan Detachment in the middle of the study area (Fig. 1). Schmidt hammer measurements of rock strength reveal uniformly strong rocks across the study area, except for some weaker units within the Tethyan series (Craddock et al., 2007).

The 10 gauged watersheds represent a range of basin areas as well as topographic and climatic conditions (Table 1). Whereas some of the watersheds in the study area are glacierized, with the area covered by glaciers ranging from 0–21% (Table 1), the dominant erosional process on the unglaciated slopes is landsliding (Burbank et al., 1996; Gabet et al., 2004a; Shroder,

1998). The region is sparsely populated and only a small proportion ($\ll 10\%$) of the area is cultivated, inhabited, or logged, thus minimizing the effects of human land-use impacts. The fluvial network is dominated by bedrock channels, with no significant storage of alluvium.

2.2. Measurements

The first monitoring station was established in 2000 on the Khudi Khola (Fig. 1); the nine others were established in the ensuing years. The establishment of the stations consisted of cross-sectional surveys and installation of stage gauges. Turbidity sensors and pressure transducers were also installed and recorded measurements to dataloggers every 30 min. To ensure the morphological stability of the cross-sections, nine of them span bedrock reaches; due to access problems, the cross-section on the Nar Khola (Fig. 1) was established across an alluvial reach. Velocities were measured at each cross-section by dropping a small plastic ball partially filled with water into the middle of the flow and timing its travel across a known distance (i.e., the “floating boat method”); the surface velocity was multiplied by 0.8 to obtain the mean cross-sectional velocity (Leopold et al., 1964). The mean flow velocity was measured at a range of discharges and, in conjunction with the cross-sectional surveys, used to develop stage-discharge rating curves for each station. Although the channels were essentially bedrock rivers, scour and fill of the bouldery beds may have resulted in some uncertainty in our estimates of discharge.

Twice daily (morning and evening) during the monsoon season (June–October), the river stage at each station was recorded and 3 water samples were collected in 500-ml bottles. Where possible, the water bottles were weighted and lowered from a bridge into the middle of the flow. Where there was no bridge, the bottles were attached to a 2-m pole and thrust as far out as possible into the flow. Because of the power of some of the rivers, the water bottles were often unable to penetrate deep

Table 1
Watershed attributes and rates

Site no. ^a	Area (km ²)	Mean elev. (m)	Mean slope (deg)	Average relief ^b (m)	Runoff (m/yr)	% Area glacierized	Average erosion rate, (range) (mm/yr) ^c	Record length (yr)
1 — Koto	812	4794	30	1076	0.76	12	1.0 (0.7–1.3)	4
2 — Nar Khola	1052	5174	28	909	0.15	10	0.1 (0.1–0.2)	3
3 — Temang Khola	21	4087	29	1070	1.62	0	0.1 (0.1–1.9)	2
4 — Danaque Khola	7	3349	32	442	1.17	0	1.0 (0.0–1.9)	2
5 — Upper Dharapani	1946	4918	26	886	0.56	11	0.4 (0.4–0.4)	3
6 — Dudh Khola	491	4694	32	1147	0.67	15	0.3 (0.2–0.5)	4
7 — Dona Khola	89 ^d	4851	32	1117	1.09	0 ^d	0.4 (0.2–0.7)	3
8 — Lower Dharapani	2605	4870	27	947	0.44	12	0.5 (0.4–0.5)	2
9 — Bhulbule	3217	4522	28	958	0.76	10	0.5 (0.4–0.6)	3
10 — Khudi Khola	152	2566	26	862	3.54	0	2.0 (1.5–3.0)	5

^a Keyed to Site nos. in Fig. 1.

^b Relief determined over a 1-km radius moving window.

^c Total erosion rate includes estimated bedload and measured solute load contributions.

^d A proglacial lake traps sediment issuing from the upper reaches of the catchment; the value shown here is the drainage area below the lake and is the area used for the erosion rate calculation. The entire catchment is 155 km² and 21% of that area is glacierized.

into the flow, thus only the top 50 cm of the water column was typically sampled. The water samples were filtered, dried, and weighed to determine sediment concentrations.

The three sediment concentrations that were collected at a given time were averaged and multiplied by water discharge to calculate sediment discharge. Sediment discharges were then integrated throughout each monsoon season to calculate an annual mass sediment yield. Although the rivers were only monitored during ~4 months each year, discharges were much lower and the water much less turbid during the remainder of the year (Fig. 3A), suggesting that we were measuring >90% of the sediment flux. Annual suspended sediment yields at each station were then averaged and used to calculate an erosion rate for the upstream contributing area.

Monitoring continued until 2004. Because of damaged and lost equipment and the staggered establishment of stations, only one station has a full 5-year record. The average record length is 3 yr and 4 stations yielded only 2 yr of data (Table 1).

2.3. Discharge calibration

Because of the difficulty in accurately gauging these rivers with our rudimentary techniques, we used satellite-based TRMM (Tropical Rainfall Measuring Mission) data (Bookhagen and Burbank, 2006) to validate our discharge measurements estimated

from the stage gauges and rating curves. The TRMM data was calibrated with ground-based precipitation data from a network of 17 weather stations distributed throughout the field area (Putkonen, 2004). From the TRMM data, we created a map of total precipitation that fell on our field site during the 2002 monsoon season. With an altitude-based model presented by Lambert and Chitrakar (1989), we created a map of potential evapotranspiration (PET) for the field site using a Geographical Information System (GIS). Assuming that the potential evapotranspiration approximates the actual evapotranspiration, we subtracted the PET from the satellite-derived precipitation to estimate net precipitation for the 2002 monsoon season. The estimated net precipitation was then used to estimate the total discharge from each watershed for the 2002 monsoon season. Finally, this calculated discharge was compared to the discharge estimated from the twice daily field measurements.

Although precipitation during the monsoon accounts for nearly all of the flow from most of the watersheds, there is an important component of glacial melt in the discharge from 3 watersheds (Nar, Koto, and Upper Dharapani). This glacial melt contribution is seen in consistent afternoon discharge peaks that are not related to rainstorms (Fig. 3B). The volume of flow contributed by glacial melt for each of the 3 watersheds was determined by integrating the discharge in these afternoon peaks; identification of these meltwater peaks was based on a

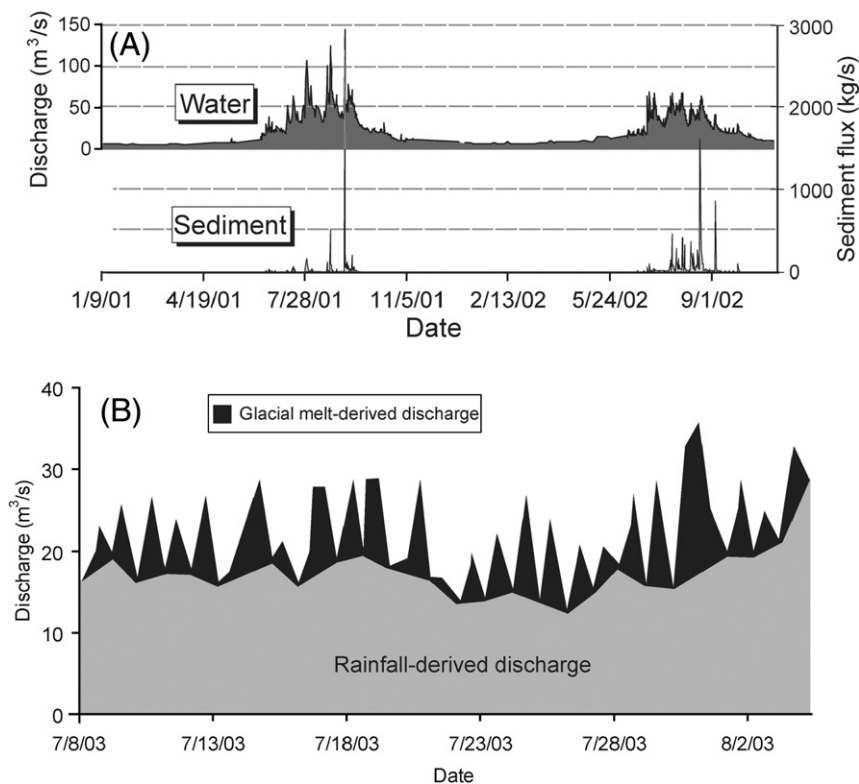


Fig. 3. (A) Two years of discharge and sediment flux data from the Khudi watershed. High discharges and sediment flux peaks are limited to the monsoon season. Note that the highest sediment flux peaks occur later in the monsoon season, emphasizing the role of prior rainfall in increasing pore water pressures and priming the landscape for larger and more frequent slope failures (Gabet et al., 2004a). (B) An example of discharge measurements from the glacierized Koto watershed. Afternoon peaks in discharge from glacier melt are evident from the twice daily stage gauge readings. The assumed glacial melt component of the total discharge is shown in black shading; the assumed rainfall-derived component is shown in grey shading.

visual examination of the hydrographs and is, therefore, subject to error. For these 3 watersheds, the glacial melt contribution was subtracted from the total discharge in order to compare the discharge measurements with the TRMM data.

3. Results

3.1. Error analysis

There are two main sources of potential errors in our erosion rate calculations: incorrect estimates of discharges and sediment concentrations. In general, the discharges calculated from the rating curves were higher than the discharges estimated from the TRMM data. For example, the average specific discharge calculated with the rating curve for the Khudi Khola is 65% higher than the amount of net precipitation that fell in that watershed. Because of these discrepancies, we used the TRMM data to calibrate the discharges measured in the field. This calibration was performed by scaling the daily discharge value by the ratio of the measured monsoon discharge to the discharge predicted from the TRMM data. For example, if the measured seasonal discharge from a watershed was 65% of the TRMM-estimated discharge, all of the daily discharge values from the monitoring stations were multiplied by $1/0.65$. Although there may be some error in this technique due to groundwater losses, these losses are likely small relative to the river discharges.

Problems related to errors in measuring sediment concentrations are more difficult to resolve than the discharge uncertainties. In particular, the sediment concentrations used in the calculations of the sediment fluxes may underestimate the vertically averaged sediment concentration. Although the particle-size distribution of the sediment captured in the sample bottles varied daily at each station, an analysis of a random selection of sediment samples suggests that 89–100% of the sediment, by mass, was smaller than 0.5 mm, with the balance of the sediment being between 0.5 and 1.5 mm. Theoretical suspended sediment concentration profiles were determined at the gauging stations using the Rouse equation (Dingman, 1984). The calculated profiles indicate that particles <0.5 mm were well-mixed throughout the water column. For particles between 0.5–1.5 mm, however, the surface concentration was undoubtedly lower than the vertically averaged sediment concentration, suggesting that total suspended sediment concentrations were somewhat underestimated. In addition, because the suspended sediment samples were taken in the mornings and late afternoons, there is the possibility that the measurements taken during these two times were not representative of the average condition. Few of the turbidity sensors survived unscathed: nearly all of them succumbed to water leakage, despite our best efforts to seal them tightly. As a result, the data from the turbidity sensors are essentially dismissed in this study. The few records that we do have, however, are useful for addressing the issue of sampling times. The sensors indicate that, typically, the highest sediment fluxes were occurring during the late night and early morning hours. Fortuitously, we find that discharges and sediment fluxes determined from the twice daily measurements and those from the sensors yield remarkably similar daily averages for both glacially-dominated and landslide-dominated watersheds.

Given the possible uncertainties, the internal consistency of the measurements can be evaluated by performing mass-balance calculations. Because the three major channels above the Lower Dharapani station (Site #8) were gauged, we can compare the sum of the flow from those tributaries to the flow past Lower Dharapani. For the 2002 monsoon season, the year with the most complete records, we find a robust correlation between the daily discharge measured at Lower Dharapani and the sum of the upstream gauges although the regression indicates that the measured discharge is slightly lower than the sum of the contributing flows (Fig. 4A). Given our use of rudimentary techniques and the practical difficulties in gauging these remote, high-gradient rivers, we consider the strong correlation of the Lower Dharapani discharges with the sum of the contributing discharges to indicate that the overall pattern and magnitude of discharge were reliably captured. For the same period, we find a reasonable 1:1

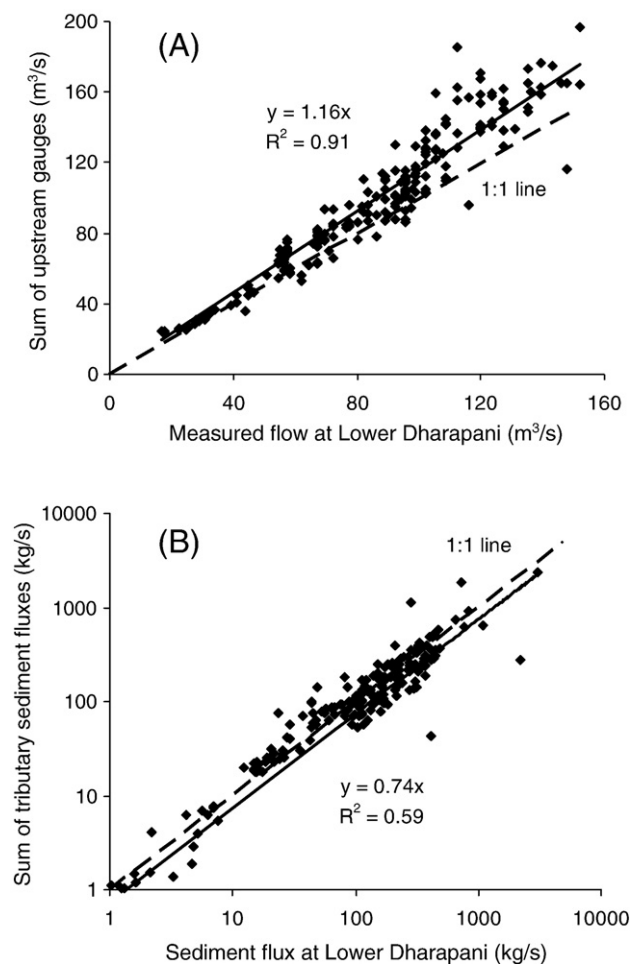


Fig. 4. (A) The close correlation between the TRMM-calibrated discharge at the Lower Dharapani station and the sum of the flows from the upstream stations suggests that the discharge rating curves are reasonably accurate. The regression (solid line) indicates, however, a slight but systematic error in which the discharge at the Lower Dharapani site is lower than the sum of the upstream stations' discharges. 1:1 line is dashed. (B) The sediment flux at the Lower Dharapani station matches reasonably well the sum of the sediment fluxes from the upstream stations over four orders of magnitude (note logarithmic axes). The rapid passage of the sediment pulses and the asynchronous timing of the sampling times account for some of the scatter. 1:1 line is dashed.

relationship between the sum of the suspended sediment flux from the tributaries and the measured sediment flux past Lower Dharapani over a range of four orders of magnitude (Fig. 4B) (note that the channels are steep and narrow and no significant fluvial sediment storage occurs in or adjacent to the channels). Because of the rapid passage of sediment pulses and the asynchronous sampling times, the comparison of the sediment fluxes displays more scatter than the water discharges. Nevertheless, the results of the two mass-balance calculations are encouraging and suggest that, at a minimum, the relative rates of erosion are being accurately characterized.

3.2. Erosion rates

To calculate total erosion rates, estimated bedload fluxes and solute fluxes must be added to the suspended sediment fluxes. Solute loads measured during the 2002 monsoon season suggest that the mass lost by chemical weathering is 1–4% of the mass lost by suspended sediment flux (Gabet et al., 2004b). To es-

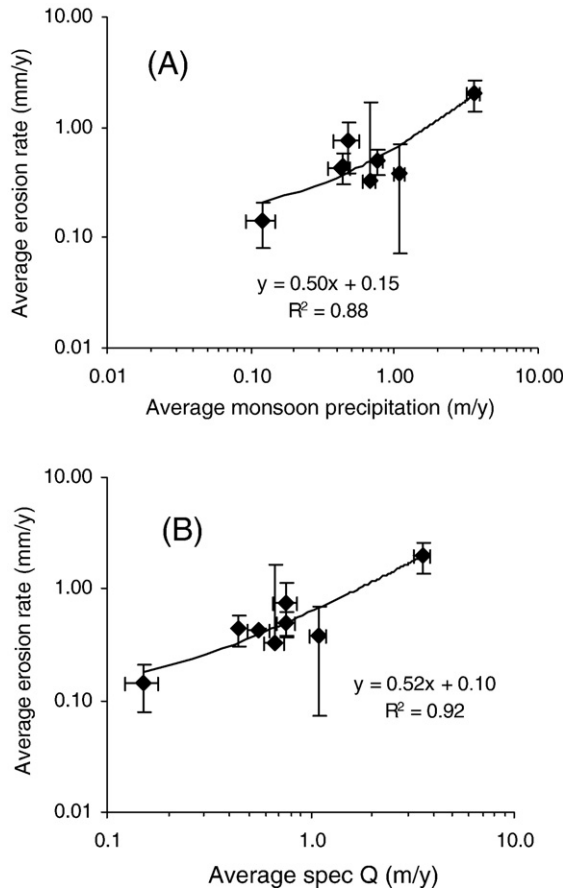


Fig. 5. (A) There is a positive relationship between net monsoon precipitation and erosion rate over nearly 2 orders of magnitude of precipitation. Error bars represent 1σ . Large error bars in erosion rates are associated with sediment records dominated by highly pulsed events that cause pronounced year-to-year variations. Overlap of two markers gives the appearance of only 7 data points, rather than the 8 plotted. (B) A positive relationship also emerges between specific discharge and erosion rate. The specific discharge includes contributions from melting ice and snow. Because specific discharge implicitly accounts for glacial activity, it may be a better predictor of erosion rate than precipitation. Note logarithmic axes on both plots.

timate bedload contributions, lacustrine and deltaic deposits from a mid-Holocene landslide-dammed lake in the northern portion of the field area were mapped (Garde et al., 2004; Pratt-Sitaula et al., 2007); this analysis determined that bedload (assumed to be the deltaic sediments) contributed $\sim 33\%$ to the total sediment yield (cf. Galy and France-Lanord, 2001). We apply this 2:1 suspended load-to-bedload ratio throughout our field site. Nevertheless, we recognize the problem inherent in applying this single value for all of the sites and address the issue later in this contribution.

The erosion rate for the Temang Khola catchment (Site #3) is considerably lower than rates for the adjacent watersheds (Table 1); this is likely due to its relatively small drainage area (21 km^2), short monitoring record (2 yr), and the impulsive nature of sediment delivery to channels due to episodic landsliding. The Danaque Khola (Site #4) drainage area is even smaller (7 km^2) and, as a result, we dismiss the erosion rates from these two catchments and only consider the rates from the remaining eight watersheds in the following analyses.

Although the data are not evenly distributed across the range of monsoon precipitation values, they suggest a positive linear relationship between effective precipitation and erosion rate (Fig. 5A). Erosion rates are also positively correlated to specific discharge, which integrates both rainfall and flow from glacial melt (Fig. 5B). In addition, all but one of the watersheds (Lower Dharapani) has positive year-to-year correlations between specific discharge and erosion (Fig. 6). Finally, erosion rates are not positively correlated with either average watershed slope nor with relief; this is not surprising considering that, for a portion of the field area, higher precipitation is associated with gentler slopes and lower relief (Gabet et al., 2004c). Similarly, Garzanti et al. (2007) found no relationship between erosion rates and relief in the region.

The relatively short monitoring periods render any conclusions regarding relationships between erosion rates and climatic and topographic factors tenuous. Although the erosion rate estimate in the Khudi Khola catchment is encouragingly similar to rates determined in other studies (Blythe et al., 2007; Brewer et al., 2006; Burbank et al., 2003; Garzanti et al., 2007; Niemi et al., 2005), short monitoring periods introduce unavoidable problems with using river data to calculate erosion rates. Short monitoring periods typically miss the very large events that happen infrequently. Conversely, rare, high-magnitude events may be recorded, but without estimates of their recurrence intervals, their role in contributing to the long-term erosion rate is unknown. The use of a set of watersheds that spans nearly 3 orders of magnitude also introduces problems that make it difficult to relate erosion rates with regional patterns of precipitation: small watersheds may bear the brunt of a particularly intense storm whereas a very large watershed may be averaging an order-of-magnitude range in annual precipitation. In addition, when landsliding is a dominant erosion process, as is typical in the Himalaya (Burbank et al., 1996), the measured sediment flux is expected to scale with catchment size and, in small catchments, to systematically underestimate long-term erosion rates (Niemi et al., 2005). Therefore, in order to compare the measured denudation with the broad pattern of precipitation,

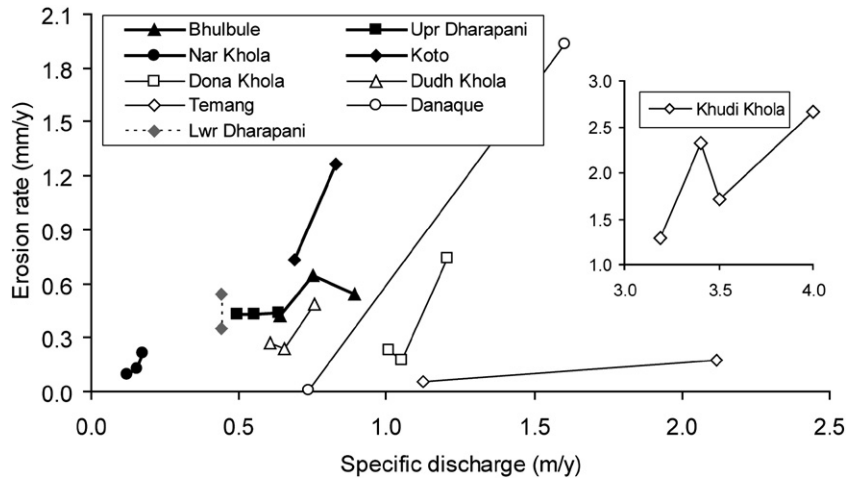


Fig. 6. Annual erosion rates in individual catchments typically increase with specific discharge (except for the Lower Dharapani, shown in gray with the dotted line). Each point represents the data for one year. Data identified with filled markers and thicker lines represent catchments > 500 km². Axis titles for inset plot are the same as for the larger plot.

erosion rates were calculated for 4 similar-sized regions in the Bhulbule watershed. Erosion rates for the Middle and Lower Marsyandi regions, both comprising partial watersheds, were determined by subtracting the sediment entering into a reach from that exiting it. Although the uncertainties are large due to this differencing technique, the results suggest a general trend of higher erosion rates in the southeastern portion of the field site and lower rates in the northwest portion (Fig. 7). This southeast-

to-northwest decrease in erosion rates parallels the dominant wind patterns in the region that bring moisture from the Bay of Bengal (Lang and Barros, 2002); as the moist air is lifted up and over the Annapurnas, orographic effects focus the highest amounts of rainfall in the southeastern portion of the field site. Although their erosion rates are higher than those found in this study, Garzanti et al. (2007) also found the highest erosion rates along the southern front of the High Himalayas.

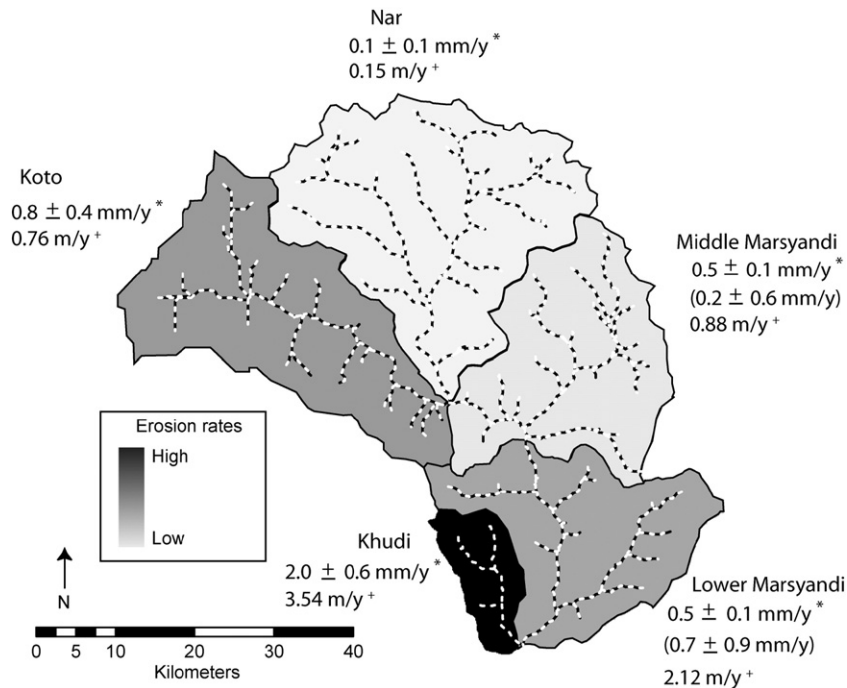


Fig. 7. Erosion rates ($\pm 1\sigma$) for areas > 600 km² and the Khudi catchment. Erosion rates with the asterisks are the rates for the entire catchment, including the upstream tributaries. For example, the asterisked erosion rate for the Middle Marsyandi includes the Nar and Koto watersheds. Erosion rates in parentheses are for the individual regions delineated in black (see text); the higher standard deviations are a result of error propagation. Mean runoff for regions delineated in black shown with a + sign. Erosion rates appear to generally decrease along a northeast transect.

4. Discussion

4.1. Controls on modern erosion rates

Attempts to relate the erosion rates measured here to topographic or climatic factors must be done carefully. In addition to the measurement uncertainties and the short monitoring periods, the landscape is most likely not at steady-state in the short-term (Pratt-Sitaula et al., 2004). The strength of the monsoon has varied significantly over time (Bookhagen et al., 2005a; Overpeck et al., 1996; Prell et al., 1992), and as noted above, some of the catchments were more extensively glacierized in the past. The effect of this history on both measured and actual erosion rates could potentially be substantial. The U-shaped valleys cut by the glaciers in the higher catchments trap hillslope-derived sediment on the low-gradient valley floor, thus decoupling the hillslopes from the channels and biasing our results towards lower erosion rates. Although we observed numerous small fans and talus cones at the base of the slopes, especially in glacierized valleys, we estimate the storage of material to be small relative to the measured sediment fluxes. Perhaps a more important legacy from the recent glaciation is its effect on the supply of sediment. As the glaciers withdraw upslope, they leave behind valley walls scoured clean of weathered and easily erodible rock and soil, unveiling a landscape where erosion is limited by the supply of transportable material. Although this may be offset somewhat by the presence of glacial deposits on the valley floor, the relatively low erosion rates in the high elevation sites suggest that the easily accessible sources have already been mined. During the strengthened early Holocene monsoon, sediment transport rates were high (Goodbred and Kuehl, 1999) and many Himalayan rivers were overwhelmed with sediment (Pratt et al., 2002), suggesting that the watersheds may have been flushed of sediment. The sediment-poor condition of the northern catchments today is supported by the

clockwise hysteretic loops in the discharge–sediment flux relationships (Fig. 8).

Given the caveats enumerated above, it appears that the current erosion rate increases with rainfall and specific discharge (Fig. 5A, B). Admittedly, the data are not evenly distributed across the range of monsoonal rainfall and thus the correlation is leveraged by the data from the driest and wettest watersheds; nevertheless, a positive trend is apparent over nearly two orders of magnitude of monsoon precipitation. Although short-term records such as these may fail to capture the average conditions, the positive correlation between precipitation and erosion found here is supported by work done by others in the region (Amidon et al., 2005; Garzanti et al., 2007). In addition, the mass-balance calculations (Fig. 4A, B) and the generally positive relationships between annual erosion and discharge recorded in each watershed (Fig. 6) suggest that, at the very least, the relative rates are reasonable.

Because the channels issuing from the studied watersheds are steep bedrock rivers, the sediment flux reflects the production of sediment from hillslope erosion. The role of precipitation in modulating the sediment supply can be addressed at two different spatial and temporal scales. At the annual scale for individual watersheds, the sediment supply increases with precipitation (Fig. 5A) because of the role of rainfall-induced increases in pore pressure in triggering landslides (Gabet et al., 2004a). In the northern glacierized watersheds, greater discharges may be associated with higher sediment fluxes due to the production of more meltwater and the extension of the subglacial hydrological network (Riihimaki et al., 2005). At the scale of 10^2 – 10^3 yr and over the entire field site, higher rates of chemical weathering (White and Blum, 1995) and biotic activity (Gabet et al., 2003) in the wetter watersheds may produce more easily erodible material.

The apparent control of present-day erosion rates by precipitation in the High Himalayas supports an important premise

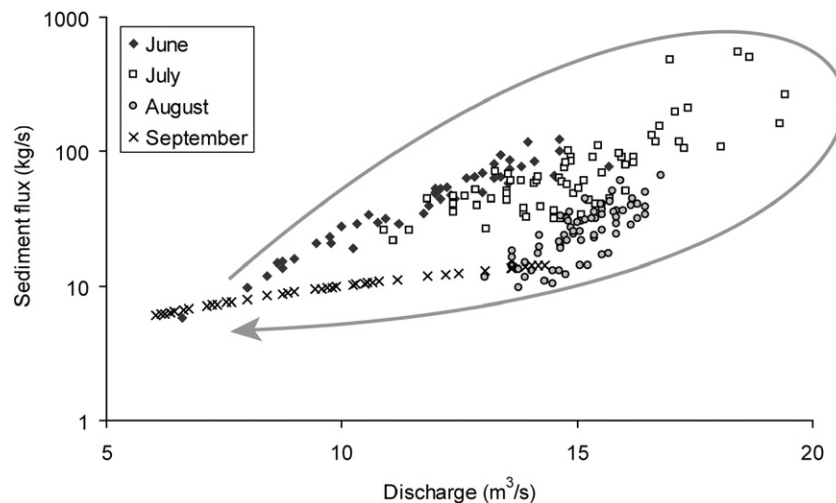


Fig. 8. Sediment flux vs. water discharge from the Nar Khola during the 2002 monsoon season. Clockwise hysteresis loop is typical of the northern glacierized watersheds in the field site. The grey arrow indicates the direction of time. The system becomes sediment-starved as the monsoon season progresses, suggesting an englacial sediment source. For clarity, peak sediment fluxes are not shown; see Fig. 9B for full data set. Y-axis is logarithmic.

in the hypothesis that precipitation, erosion, and uplift are linked via a feedback loop (Beaumont et al., 2001; Hodges et al., 2001; Hodges et al., 2004). Hodges et al. (2004) and Wobus et al. (2003) have suggested that, at present, high rock uplift rates in the region are spatially correlated with the zone of highest rainfall. The data that we present here suggest that the catchment with the highest erosion rate is also spatially correlated with the highest rainfall rates, the hanging wall of the Main Central Thrust (which was active during the Quaternary: Huntington et al., 2006), and the southern flank of the High Himalayas (Fig. 7), thus potentially closing the feedback loop.

4.2. Modern erosion rates vs. long-term erosion rates

Paradoxically, erosion rates measured at time scales of 10^5 – 10^6 yr suggest that rates of rock uplift and erosion are insensitive to the steep precipitation gradient (Blythe et al., 2007; Burbank et al., 2003). For example, despite the 10-fold rainfall gradient across the study area, spatially uniform apatite fission-track ages imply similarly uniform erosion rates of 2–5 mm/yr over the last 0.5–1.0 Myr (Blythe et al., 2007; Burbank et al., 2003; Whipp et al., 2007). Although our sediment flux-based rate for the Khudi watershed agrees with these long-term rates, the rates measured here for the rest of the study area are 4–20 times lower than the long-term denudation rates (Fig. 7). This difference raises the question of whether we are underestimating long-term erosion rates when using modern river data.

In addition to the sources of uncertainty noted above, other sources of error could lead to an underestimate of erosion rates. First, the bedload flux may be underestimated. Although our suspended load:bedload ratio is locally derived (Garde et al., 2004; Pratt-Sitaula et al., 2007), Galy and France-Lanord (2001) suggest that bedload fluxes in the Himalayas may be of the same magnitude as suspended sediment fluxes. If this were the case for our study area, the modern erosion rates (excluding Khudi) would range from 0.2–1.1 mm/yr, yet would still remain lower than the long-term rates (Blythe et al., 2007; Burbank et al., 2003; Whipp et al., 2007). In fact, a suspended load:bedload ratio of 1:4 would be needed to produce modern erosion rates similar to the long-term rates, a value that is well beyond the range of previous estimates (Galy and France-Lanord, 2001; Garde et al., 2004; Pratt-Sitaula et al., 2007). Moreover, based on this supposition, the southeast-to-northwest decrease in modern rates would still exist: the rates would simply be higher unless the fraction of bedload systematically increased from south to north. Another source of error may be that our estimates of river flow are too low. By calibrating our field-based discharge measurements with the TRMM data, we are confident that our discharge estimates are approximately correct; revising our discharge measurements upwards would imply that more water is leaving the watersheds than is entering, even after accounting for reasonable rates of glacial melt. In addition, our mass-balance calculations suggest that our discharge measurements are sufficiently reliable to permit meaningful comparisons among stations (Fig. 4A).

It might also be argued that erosion rates in the northeast are underestimated due to a mismatch between the frequency of

large erosional events and the sampling duration. In addition to glacial activity, erosion in the drier, northern watersheds may also occur by rare, deep-seated landslides that were not captured during the short monitoring period (Bookhagen et al., 2005b; Weidinger, 2006), but which could potentially contribute the bulk of the sediment flux (Hovius et al., 1997). Our field observations suggest, however, that deposits from deep-seated failures along the length of the Marsyandi River are roughly uniformly distributed and do not appear to be concentrated in the north. Finally, we note that a single, large debris flow in the northern catchment of the Dudh Khola in 2003 (a rare occurrence according to the local population) doubled the calculated erosion rate for that watershed, but only brought it up to 0.3 mm/yr, still less than the long-term rate of 2–5 mm/yr (Blythe et al., 2007; Burbank et al., 2003).

To reconcile the general present-day trend of low erosion rates in the north and high rates in the south with the high, spatially uniform long-term rates (Blythe et al., 2007; Burbank et al., 2003; Whipp et al., 2007), we examine the spatial distribution of erosional intensities and regimes. Erosion in the southern, landslide-dominated watersheds may be approximately steady across several temporal scales; this is supported by the similar rates measured for the Khudi catchment over three different time scales: 10^0 – 10^1 yr (this study), 10^2 – 10^3 yr (Niemi et al., 2005), and 10^5 – 10^6 yr (Blythe et al., 2007; Burbank et al., 2003; Whipp et al., 2007). In contrast, the rate of erosion in the high elevation northern watersheds likely oscillates between extremes. Although the high elevation regions of these watersheds are presently glacierized, glaciers were far more extensive in the past (Duncan et al., 1998; Fort, 1986; Pratt-Sitaula et al., 2005). For example, glacial striae and other geomorphic features suggest that valley glaciers may have descended down the entire length of the Dudh (Site #6) and Dona Khola (Site #7) watersheds, nearly reaching the junction with the Marsyandi. A valley glacier likely also reached down the upper Marsyandi to its junction with the Nar Khola. At present, the lower reaches of these three valleys are ice-free and glaciers can only be found in the headwaters of their catchments. Because glaciers are generally considered to be highly efficient agents of erosion (Hallet et al., 1996; Mitchell and Montgomery, 2006; Naylor and Gabet, 2007; Oskin and Burbank, 2005), denudation rates in these northern watersheds during glacial periods likely outpace the rates in the lower, unglaciated (or slightly glaciated) southern watersheds. Conversely, during interglacials, the glaciers retreat and under the generally drier conditions of the north, erosion slows dramatically. Therefore, although erosion rates are high during glacial periods, the prolonged pause during the interglacials may lead to a time-averaged erosion rate in the higher elevation sites that matches the rate of the wetter, non-glaciated regions in the south, producing the long-term spatially uniform rates documented by others (Blythe et al., 2007; Burbank et al., 2003). Given this hypothesis, it is reasonable to ask why the non-glacial landscape to the south should be eroding at the same rate as the glaciated landscape to the north. We propose that, at the time-scale of 10^5 – 10^6 yr, rock uplift may be balanced by erosion throughout the entire region as southern Tibet is laterally advected over a

crustal-scale ramp (Bollinger et al., 2006; Burbank et al., 2003). Recent modeling of coupled tectonic and surface processes of the central Nepalese Himalaya (Godard et al., 2006) showed low sensitivity to the spatial distribution of rainfall but high sensitivity to the underlying structural geometry, spatial variations in rock strength, and the total amount of rainfall.

In the lower, southern portion of the field area, hillslopes appear to be at their threshold angle for failure (Gabet et al., 2004c), and the absence of floodplains tightly couples the hillslopes to the channel network. As the relative baselevel of the Marsyandi drops (due to regional uplift), incision propagates up the channel network, destabilizing the toes of hillslopes and triggering landslides. In this way, rock uplift is matched by erosion from the bottom up such that steady-state conditions are imposed by the lower boundary (Burbank, 2002; Burbank et al., 1996). In contrast, in the northern, glaciated catchments, we speculate that steady-state is imposed from the top down. As the mountains are pushed skyward, the mean heights of mountain ranges are modulated by the elevation of the equilibrium-line altitude, where the greatest ice flux and fastest erosion is inferred to occur (i.e., the “glacial buzzsaw”) (Broecker and

Denton, 1990; Brozovic et al., 1997; Humphrey and Raymond, 1994; Mitchell and Montgomery, 2006). Faster rock uplift rates lead to more terrain at higher elevations thus allowing for more ice and snow accumulation. Greater volumes of ice and snow produce more and larger glaciers that can drive erosion rates that match and, for short periods, exceed rock uplift rates. We note that in the northern Marsyandi catchment, only a small fraction of the area lies above 6500 m elevation. As such, the effectiveness of glacial erosion is not significantly limited either by being cold-based and frozen to their beds (i.e., not eroding) or by lying within the arid zone proposed for regions >6200 m (Harper and Humphrey, 2003).

The role of glaciations in accelerating erosion rates in the region during the Pliocene can be explored by estimating the amount of bedrock lowering presently being accomplished by glaciers. The discharge and sediment flux records from the northern watersheds demonstrate a clockwise hysteretic relationship between discharge and sediment flux whereby sediment fluxes are high during the early monsoon but decrease later in the season (Fig. 8). Others have also observed a similar relationship from glacially fed channels and Riihimaki et al. (2005) reasoned

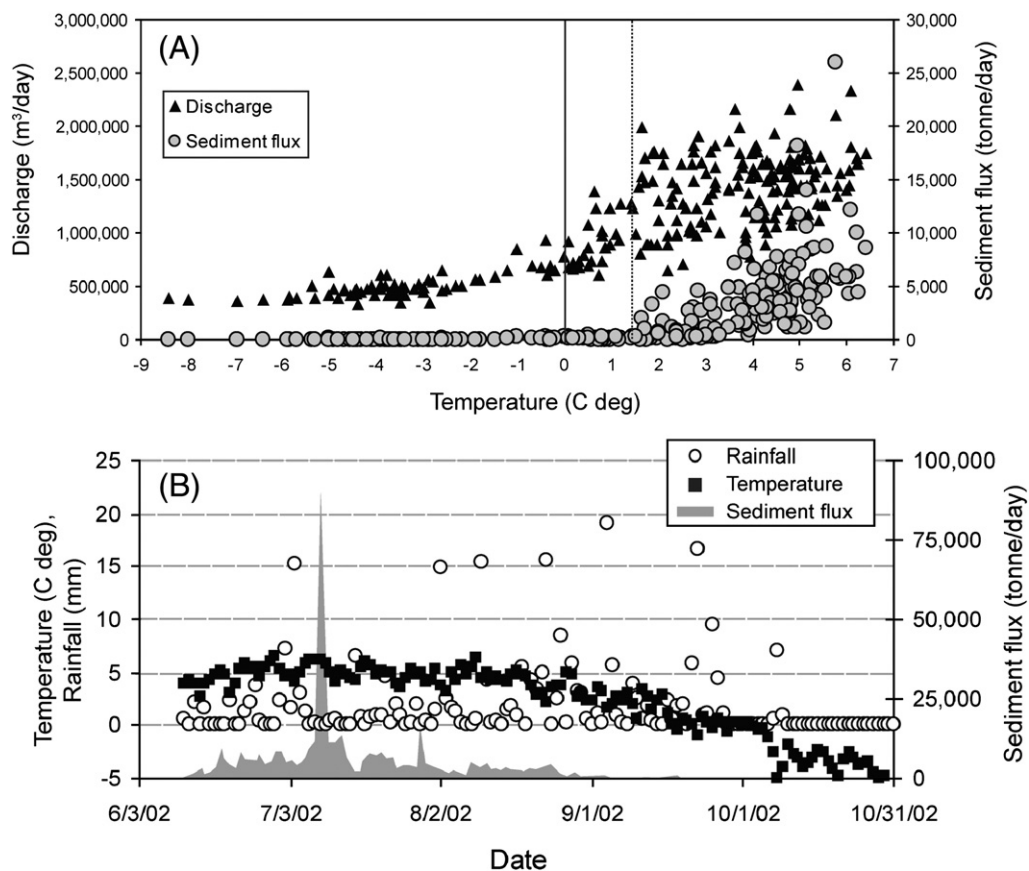


Fig. 9. (A) Higher discharges on the Nar Khola were recorded as the mean daily temperature at the snout of the glaciers increased above freezing (solid line). Temperatures above 1.5 °C (dotted line) are associated with higher sediment fluxes, suggesting a subglacial sediment source. Temperatures were recorded at an elevation of 4220 m; temperatures at the snout of the glaciers (elev. ~5200 m) were estimated using a lapse rate of 5 °C/km (Pratt-Sitaula, 2005). Data from 2001, 2002 monsoon seasons; for clarity, peak sediment fluxes are not shown. (B) High sediment fluxes from the Nar Khola watershed occur during the early part of the monsoon season (2002) when the mean daily temperatures are the highest; significant sediment flux was only measured when temperatures were above ~3 °C. In contrast, the higher amounts of precipitation recorded later in the season are not associated with high sediment fluxes. The dependence of sediment flux on temperature strongly suggests a subglacial sediment source.

that the hysteresis was due to a flushing of subglacial sediment (see also Willis et al., 1996). Although our monitoring stations were tens of kilometers from the glaciers, the suspended sediment signal strongly suggests that the chronic sources of sediment to the channels are the presently glacierized areas. The dependence of discharge and sediment flux on temperature (Fig. 9A) also argues in favor of modern glaciers being an important sediment source in the northern catchments. Higher discharges and sediment fluxes appear to be associated with threshold temperatures at the snout of the glaciers (Fig. 9A); as the warmer temperatures move upslope and reach the glaciers, meltwater is produced and the subglacial hydrological network may extend into pockets of stored sediment (Riihimaki et al., 2005). In addition, high sediment fluxes coincide with warmer temperatures rather than higher rainfall (Fig. 9B), another indication that the sediment is being produced from the glacierized regions. In contrast, in the landslide-dominated southern catchments, the suspended sediment signal is clearly due to the storm-driven delivery of sediment from landslides, and no evidence exists of a clockwise hysteretic relationship between discharge and sediment flux during the monsoon season (Gabet et al., 2004a). Indeed, sediment fluxes in the landslide-dominated catchments increase during the monsoon as the slopes become progressively wetter and unstable (Fig. 3A). Therefore, with the inference that the predominant sources of sediment in the northern catchments are the currently glacierized areas, the erosion rates due to glaciers may be roughly estimated by dividing the modern watershed-scale erosion rates by the fraction of ice-covered area (Table 1). With this approach, the glacial erosion rates in the northernmost watersheds are estimated as 4.8 mm/yr for the Nar catchment and 3.8 mm/yr for the Dudh Khola catchment, similar to rates measured by Gardner and Jones (1993) for glacial erosion in the Nanga Parbat region of the Himalayas. These values suggest that rapid erosion during glacial advances in the northern catchments could compensate for low interglacial erosion to produce a time-averaged rate that may match the erosion rates measured in the landslide-dominated southern catchments.

5. Conclusion

Hypotheses on the relationships between climate, erosion, and tectonics hinge on the spatial distributions of precipitation and erosion. It has been proposed that intense monsoonal rainfall at the Himalayan front has driven high erosion rates that localize tectonic strain. Long-term exhumation rates (10^5 – 10^6 yr) measured in central Nepal, however, appear quite independent of modern climate gradients at spatial scales of tens of kilometers. Through quantification of variations in suspended sediment loads across the Himalaya, we show that spatial gradients in modern erosion rates parallel modern monsoon rainfall rates. Thus, in contrast to the high, spatially uniform, long-term denudation rates documented by others, we find high erosion rates in the low-elevation, wet, southern watersheds and low rates in the high elevation, arid, northern watersheds. We propose that at longer time scales ($>10^4$ yr), rapid but intermittent erosion by glaciers in the northern watersheds balances the more

steady erosion in the landslide-dominated southern watersheds such that, over time, the entire region is being eroded at approximately the same rate.

Acknowledgments

This research was supported by the National Science Foundation Continental Dynamics program (grant EAR-9909647) and by the National Aeronautics and Space Administration (NAGS-7781, NAGS-9039, NAGS-10520). Invaluable logistical support from Himalayan Experience enabled collection of meteorological and discharge data. The Nepalese Department of Hydrology and Meteorology is gratefully acknowledged for their help and cooperation. D. Malmon and an anonymous reviewer are thanked for their comments and suggestions.

References

- Aalto, R., Dunne, T., Guyot, J.L., 2006. Geomorphic controls on Andean denudation rates. *J. Geol.* 114, 85–99.
- Amidon, W.H., Burbank, D.W., Gehrels, G.E., 2005. U–Pb zircon ages as a sediment mixing tracer in the Nepal Himalaya. *Earth Planet. Sci. Lett.* 235, 244–260.
- Barros, A.P., Joshi, M., Putkonen, J., Burbank, D.W., 2000. A study of the 1999 monsoon rainfall in a mountainous region in central Nepal using TRMM products and rain gauge observations. *Geophys. Res. Lett.* 27, 3683–3686.
- Beaumont, C., Jamieson, R.A., Nguyen, M.H., Lee, B., 2001. Himalayan tectonics explained by extrusion of a low-viscosity crustal channel coupled to focused surface denudation. *Nature* 414, 738–742.
- Blythe, A.E., Burbank, D.W., Carter, A., Schmidt, K., Putkonen, J., 2007. Plio-Quaternary exhumation history of the central Himalaya: 1. Apatite and zircon fission-track and apatite [U–Th]/He data. *Tectonics* 26, TC3002. doi:10.1029/2006TC001990.
- Bollinger, L., Henry, P., Avouac, J.P., 2006. Mountain building in the Nepal Himalaya: thermal and kinematic model. *Earth Planet. Sci. Lett.* 244, 58–71.
- Bookhagen, B., Burbank, D.W., 2006. Topography, relief, and TRMM-derived rainfall variations along the Himalaya. *Geophys. Res. Lett.* 33. doi:10.1029/2006GL026037.
- Bookhagen, B., Thiede, R.C., Strecker, M.R., 2005a. Abnormal monsoon years and their control on erosion and sediment flux in the high, arid northwest Himalaya. *Earth Planet. Sci. Lett.* 231, 131–146.
- Bookhagen, B., Thiede, R.C., Strecker, M.R., 2005b. Late Quaternary intensified monsoon phases control landscape evolution in the northwest Himalaya. *Geology* 33 (2), 149–152.
- Brewer, I.D., Burbank, D.W., Hodges, K.V., 2006. Downstream development of a detrital cooling-age signal: insights from Ar40/Ar39 muscovite thermochronology in the Nepalese Himalaya. In: Willet, S.D., Hovius, N., Brandon, M.T., Fisher, D.M. (Eds.), *Tectonics, Climate, and Landscape Evolution: GSA Special Paper 398*. Geological Society of America, pp. 321–338.
- Broecker, W.S., Denton, G.H., 1990. What drives glacial cycles? *Sci. Am.* 262, 48–56.
- Brozovic, N., Burbank, D.W., Meigs, A.J., 1997. Climatic limits on landscape development in the northwestern Himalaya. *Science* 276, 571–574.
- Burbank, D.W., 2002. Rates of erosion and their implications for exhumation. *Mineral. Mag.* 66 (1), 25–52.
- Burbank, D.W., Blythe, A.E., Putkonen, J.L., Pratt-Sitaula, B.A., Gabet, E.J., Oskin, M.E., Barros, A.P., Ohja, T.P., 2003. Decoupling of erosion and climate in the Himalaya. *Nature* 426, 652–655.
- Burbank, D.W., Leland, J., Fielding, E., Anderson, R.S., Brozovic, N., Reid, M.R., Duncan, C., 1996. Bedrock incision, rock uplift and threshold slopes in the northwestern Himalayas. *Nature* 379, 505–510.
- Colchen, M., Le Fort, P., Pecher, A., 1986. Annapurna — Manaslu — Ganesh Himal. Centre National de la Recherche Scientifique, pp. 75–136.

- Craddock, W.H., Burbank, D.W., Bookhagen, B., Gabet, E.J., 2007. Bedrock channel geometry along an orographic precipitation gradient in the upper Marsyandi River valley in central Nepal. *J. Geophys. Research-Earth Surf.* 112, F03007. doi:10.1029/2006JF000589.
- Dingman, S.L., 1984. *Fluvial Hydrology*. Freeman, New York.
- Duncan, C.C., Klein, A.J., Masek, J.G., Isacks, B.L., 1998. Comparison of Late Pleistocene and modern glacier extents in central Nepal based on digital elevation data and satellite imagery. *Quat. Res.* 49, 241–254.
- Fort, M.B., 1986. Glacial extension and catastrophic dynamics along the Annapurna Front, Nepal Himalaya. In: Khule, M. (Ed.), *Proc. Symposium uber Tibet und Hochasien*, Goettinger-Geographische-Abhandlungen, Univ. de Paris Nord, pp. 105–121.
- Gabet, E.J., Burbank, D.W., Putkonen, J., Pratt-Situala, B.A., Ohja, T.P., 2004a. Rainfall thresholds for landsliding in the Himalayas of Nepal. *Geomorphology* 63, 131–143.
- Gabet, E.J., Langner, H., Burbank, D.W., 2004b. Geomorphic controls on chemical weathering rates in the High Himalayas of Nepal. *EOS Transactions AGU* 85(47), Fall Meeting Supplement.
- Gabet, E.J., Pratt-Situala, B.A., Burbank, D.W., 2004c. Climatic controls on hillslope angle and relief in the Himalayas. *Geology* 32 (7), 629–632.
- Gabet, E.J., Reichman, O.J., Seabloom, E., 2003. The effects of bioturbation on soil processes and sediment transport. *Ann. Rev. Earth Planet. Sci.* 31, 259–273.
- Galy, A., France-Lanord, C., 2001. Higher erosion rates in the Himalaya: geochemical constraints on riverine fluxes. *Geology* 29 (1), 23–26.
- Garde, M., Pratt-Situala, B.A., Burbank, D.W., Oskin, M., Heimsath, A., 2004. Triple whammy: Mid-Holocene landslide dam yields suspended load-bedload ratio, regional erosion rate, and bedrock incision rate, central Nepal Himalaya. *Eos Trans AGU* 85 (47) Fall Meet. Suppl., Abstract T31B-1307.
- Gardner, J.S., Jones, N.K., 1993. Sediment transport and yield at the Raikot Glacier, Nanga Parbat, Punjab Himalaya. In: Shroder Jr., J.F. (Ed.), *Himalaya to the Sea*. Routledge, London, pp. 184–197.
- Garzanti, E., Vezzoli, G., Ando, S., Lave, J., Attal, M., France-Lanord, C., DeCelles, P., 2007. Quantifying sand provenance and erosion (Marsyandi River, Nepal Himalaya). *Earth Planet. Sci. Lett.* 258, 500–515.
- Godard, V., Lave, J., Cattin, R., 2006. Numerical modeling of erosion processes in the Himalaya of Nepal: effects of spatial variations of rock strength and precipitation. In: Buitter, S.J.H., Schreurs, G. (Eds.), *Analogue and numerical modeling of crustal-scale processes*. Geological Society of London, London, pp. 341–358.
- Goodbred, S.L.J., Kuehl, S.A., 1999. Holocene and modern sediment budgets for the Ganges–Brahmaputra river system: evidence for highstand dispersal to floodplain, shelf, and deep-sea depocenters. *Geology* 27, 559–562.
- Hallet, B., Hunter, L., Bogen, J., 1996. Rates of erosion and sediment evacuation by glaciers: a review of field data and their implications. *Glob. Planet. Change* 12, 213–235.
- Harper, J., Humphrey, N.F., 2003. High altitude Himalayan climate inferred from glacial ice flux. *Geophys. Res. Lett.* 30, 1764. doi:10.1029/2003GL017329.
- Hodges, K.V., Hurtado, J.M., Whipple, K.X., 2001. Southward extrusion of Tibetan crust and its effect on Himalayan tectonics. *Tectonics* 20 (6), 799–809.
- Hodges, K.V., Wobus, C., Ruhl, K., Schildgen, T., Whipple, K., 2004. Quaternary deformation, river steepening, and heavy precipitation at the front of the Higher Himalayan ranges. *Earth Planet. Sci. Lett.* 220, 379–389.
- Hovius, N., Stark, C.P., Allen, P.A., 1997. Sediment flux from a mountain belt derived by landslide mapping. *Geology* 25 (3), 231–234.
- Humphrey, N.F., Raymond, C.F., 1994. Hydrology, erosion, and sediment production in a surging glacier: the Variegated Glacier surge, 1982–1983. *J. Glaciol.* 40, 539–552.
- Huntington, K.W., Blythe, A.E., Hodges, K.V., 2006. Climate change and Late Pliocene acceleration of erosion in the Himalaya. *Earth Planet. Sci. Lett.* 252 (1–2), 107–118.
- Lambert, L., Chitrakar, B.D., 1989. Variation of potential evapotranspiration with elevation in Nepal. *Mt. Res. Dev.* 9 (2), 145–152.
- Lang, T.J., Barros, A.P., 2002. An investigation of the onsets of the 1999 and 2000 monsoons in central Nepal. *Mon. Weather Rev.* 130, 1299–1316.
- Leopold, L.B., Wolman, M.G., Miller, J.P., 1964. *Fluvial Processes in Geomorphology*. W. H. Freeman and Co., San Francisco.
- Milliman, J.D., Syvitski, J.P.M., 1992. Geomorphic/tectonic control of sediment discharge to the ocean: the importance of small mountainous rivers. *J. Geol.* 100, 525–544.
- Mitchell, S.G., Montgomery, D.R., 2006. Influence of a glacial buzzsaw on the height and morphology of the Cascade Range in central Washington State, USA. *Quat. Res.* 65, 96–107.
- Montgomery, D.R., Brandon, M.T., 2002. Topographic controls on erosion rates in tectonically active mountain ranges. *Earth Planet. Sci. Lett.* 201, 481–489.
- Naylor, S., Gabet, E.J., 2007. Valley asymmetry and glacial vs. non-glacial erosion in the Bitterroot Range, Montana, USA. *Geology* 35 (4), 375–378.
- Niemi, N.A., Oskin, M.E., Burbank, D.W., Heimsath, A.M., Gabet, E.J., 2005. Effects of bedrock landslides on cosmogenically determined erosion rates. *Earth Planet. Sci. Lett.* 237, 480–498.
- Oskin, M., Burbank, D.W., 2005. Alpine landscape evolution dominated by cirque retreat. *Geology* 33, 933–936.
- Overpeck, J., Anderson, D.M., Trumbore, S., Prell, W.L., 1996. The Southwest Indian monsoon over the last 18000 years. *Clim. Dyn.* 12, 213–225.
- Pratt, B.A., Burbank, D.W., Putkonen, J., Ohja, T.P., 2002. Impulsive alluviation during early Holocene strengthened monsoons, central Nepal Himalaya. *Geology* 30 (10), 911–914.
- Pratt-Situala, B.A., 2005. *Glaciers, climate, and topography in the Nepalese Himalaya*, University of California, Santa Barbara.
- Pratt-Situala, B.A., Burbank, D.W., Heimsath, A., Ohja, T.P., 2004. Landscape disequilibrium on 1000–10,000 year scales Marsyandi River, Nepal, central Himalaya. *Geomorphology* 58, 223–241.
- Pratt-Situala, B.A., Burbank, D.W., Heimsath, A.M., Humphrey, N., Oskin, M., Putkonen, J., 2005. Climate and glaciation in the Nepalese Himalaya. *Eos Trans AGU* 86 (52) Fall Meeting Suppl., Abstract H51C-0381.
- Pratt-Situala, B.A., Garde, M., Burbank, D.W., Oskin, M., Heimsath, A., Gabet, E.J., 2007. Bedload-to-suspended load ratio and rapid bedrock incision from Himalayan landslide-dam lake record. *Quat. Res.* 68, 111–120.
- Prell, W.L., Murray, S.C., Anderson, D.M., 1992. Evolution and variability of the Indian Ocean summer monsoon: Evidence from the western Arabian Sea drilling program. In: Duncan, R.A. (Ed.), *Synthesis of Results from Scientific Drilling in the Indian Ocean*. American Geophysical Union, Washington, D.C., pp. 447–469.
- Putkonen, J., 2004. Continuous snow and rain data at 500 to 4400 m altitude near Annapurna, Nepal, 1999–2001. *Arct. Antarct. Alp. Res.* 36 (2), 244–248.
- Reiners, P.W., Ehlers, T.A., Mitchell, S.G., Montgomery, D.R., 2003. Coupled spatial variations in precipitation and long-term erosion rates across the Washington Cascades. *Nature* 426, 645–647.
- Riebe, C.S., Kirchner, J.W., Granger, D.E., Finkel, R.C., 2001. Minimal climatic control on erosion rates in the Sierra Nevada, California. *Geology* 29 (5), 447–450.
- Riihimaki, C.A., MacGregor, K.R., Anderson, R.S., Anderson, S.P., Loso, M.G., 2005. Sediment evacuation and glacial erosion rates at a small alpine glacier. *J. Geophys. Res.* 110. doi:10.1029/2004JF000189.
- Ruhl, K.W., Hodges, K.V., 2005. The use of detrital mineral cooling ages to evaluate steady state assumptions in active orogens: an example from the central Nepalese Himalaya. *Tectonics* 24, TC4015. doi:10.1029/2004TC001712.
- Schaller, M., von Blackenburg, F., Hovius, N., Kubik, P.W., 2001. Large-scale erosion rates from in situ-produced cosmogenic nuclides in European river sediments. *Earth Planet. Sci. Lett.* 188, 441–458.
- Searle, M.P., Godin, L., 2003. The south Tibetan detachment and the Manaslu leucogranite: a structural reinterpretation and restoration of the Annapurna–Manaslu Himalaya, Nepal. *J. Geol.* 111, 505–523.
- Shroder Jr., J.F., 1998. Slope failure and denudation in the western Himalaya. *Geomorphology* 26 (1–3), 81–105.
- Thiede, R.C., Bookhagen, B., Arrowsmith, J.R., Sobel, E.R., Strecker, M.R., 2004. Climatic control on rapid exhumation along the Southern Himalayan Front. *Earth Planet. Sci. Lett.* 222, 791–806.
- Vance, D., Bickle, M., Ivy-Ochs, S., Kubik, P.W., 2003. Erosion and exhumation in the Himalaya from cosmogenic isotope inventories of river sediments. *Earth Planet. Sci. Lett.* 206, 273–288.
- Weidinger, J.T., 2006. Predisposition, failure and displacement mechanisms of large rockslides in the Annapurna Himalayas. *Eng. Geol.* 83, 201–206.

- Whipp, D.M.J., Ehlers, T.A., Blythe, A.E., Huntington, K.W., Hodges, K.V., Burbank, D.W., 2007. Plio-Quaternary exhumation history of the central Himalaya: 2. Thermokinematic model of the thermochronometer exhumation. *Tectonics* 26, TC3003. doi:10.1029/2006TC001991.
- White, A.F., Blum, A.E., 1995. Effects of climate on chemical weathering in watersheds. *Geochim. Cosmochim. Acta* 59 (9), 1729–1747.
- Willis, I.C., Richards, K.S., Sharp, M.J., 1996. Links between proglacial stream suspended sediment dynamics, glacier hydrology and glacier motion at Middalsbreen, Norway. *Hydrol. Process.* 10, 629–648.
- Wobus, C., Hodges, K.V., Whipple, K., 2003. Has focused denudation sustained active thrusting at the Himalayan topographic front? *Geology* 31 (10), 861–864.